



TITLE:

# Properties of the Stress Field in and around West China Derived from Earthquake Mechanism Solutions

AUTHOR(S):

Xu, Jiren; ZHAO, Zhixin; ISHIKAWA, Yuzo; OIKE, Kazuo

---

CITATION:

Xu, Jiren ...[et al]. Properties of the Stress Field in and around West China Derived from Earthquake Mechanism Solutions. Bulletin of the Disaster Prevention Research Institute 1988, 38(2): 49-78

ISSUE DATE:

1988-06

URL:

<http://hdl.handle.net/2433/124953>

RIGHT:

## Properties of the Stress Field in and around West China Derived from Earthquake Mechanism Solutions

By Jiren XU, Zhixin ZHAO, Yuzo ISHIKAWA and Kazuo OIKE

(Manuscript received March 7, 1988)

### Abstract

The properties of the stress field in the West China region has been analyzed based on the 174 new solutions of focal mechanism of earthquakes with magnitudes (Mb) from 4.5 to 6.2 and the earthquake generating stress field from smoothed radiation patterns using more than 5000 initial motions of P waves of 169 earthquakes in the six concerned regions. Almost all events discussed in this paper were shallow ones. These data were obtained from the Bulletin of the International Seismological Center during the period from 1971 to 1980.

The main results are as follows: In the West China region, the compressional axes mostly lie in N-S and NE-SW directions, and the tensional axes mostly lie in E-W and NW-SE directions. This general view of the distribution of the stresses over a wide area suggests that there is the transmission of tectonic forces from the collision between the Indian plate and the Eurasian plate along the Himalayan mountains through the Tibetan plateau.

In the Himalayan mountains, along the margins of the Tibetan plateau and in the northwestern China regions, earthquakes caused by reverse faulting and strike-slip faulting are predominant.

A lot of events with normal faults are concentrated in the western and central area of the Tibetan plateau with elevations higher than 5000 m. It shows that the tensional forces in the WNW-ESE direction are predominant in this region.

The directions of P-axes and T-axes are not so simple along the margins of microplates as are those in their inner part.

Comparing various geological and geophysical data, the reason for the generation of such distribution of stress fields was discussed.

### 1. Introduction

One of important characteristics of the seismic activity in China is that the seismic regions can be divided into two parts on the large scale from the viewpoint of tectonics. The eastern part and the western part of China are bordered by the North-South Seismic Belt as a clear boundary. The western part of China, including the Himalayan region and the Tibetan plateau region, is one of the most active seismic regions in the world. In particular, it is the important region for the study of continental seismicity.

Many seismologists have reported significant results on seismicity, seismo-tectonics and so on in this region (Huan et al., 1979,<sup>1)</sup> Teng et al., 1987,<sup>2)</sup> and Shi et al., 1983<sup>3)</sup>). After studying the seismicity and the distribution of fault plane solutions, Oike (1984) suggested that the stress field in the northwestern part of China was related to the relative movement between the Indian plate and the Eurasian plate.<sup>4)</sup> Many results indicated that not only the spatial distribution of earthquakes but also the temporal

variation of the seismic activity in the Tibetan plateau region and its vicinity are related to each other by the collision of the Indian and Eurasian plates (Tapponnier and Molnar, 1977,<sup>5)</sup> Valdiya, 1981,<sup>6)</sup> Ni and Barazangi, 1984,<sup>7)</sup> Lyon-Caen and Molnar, 1983,<sup>8)</sup> Khattri, 1987,<sup>9)</sup> and Zhao et al., 1988<sup>10)</sup>). Zonenshain and Savostin (1981) pointed out that the tectonic forces caused by the collision between Indian plate and Eurasian plate affected the Baikal rift zone, transmitting through the West China and the Mongolian regions.<sup>11)</sup> These studies of the seismic activity suggest that analyses of fault plane solutions of earthquakes and related phenomena are especially significant for the seismotectonic studies of these regions.

A lot of focal mechanism solutions were reported by Verma and Krishna Kumar (1987)<sup>12)</sup>, Oike (1984)<sup>13)</sup>, Ishikawa (1986)<sup>14)</sup> and Yan et al. (1979)<sup>15)</sup>. Although the seismicity in the Himalayan, the Aaraka-Yoma and the Hindukush regions has been discussed in these studies, detailed studies of tectonics in West China have not yet been carried out. Therefore, the general tectonic view of the West China region including the whole Himalayan region, the Tibetan plateau region and the northwestern region of China has not yet been clarified.

In this paper, we study the focal mechanisms and the characteristics of the tectonics and the stress field from the Tibetan plateau region to the Baikal lake region. The area concerned in this study is located from latitude 22°N to 58°N and longitude from 77°E to 110°E. This wide area includes the Himalayan mountains, the Tibetan plateau, the Tianshan mountains, Altay mountains and some other seismically active regions. In this area, the crustal movements are violent and many large earthquakes with *M* of more than or equal to 8 have occurred frequently. The stress fields are discussed mainly based on a lot of focal mechanism solutions of large and moderate earthquakes which have occurred there. Then we are going to discuss some fundamental problems involving the tectonic force system and its relation to the stress fields in the regions concerned.

## 2. Data and methods of analyses

The reference for the data used in this paper were mainly obtained from the Bulletin of the International Seismological Center. The data of large and moderate earthquakes from 1971 to 1980 were selected from the Bulletins. The regions analyzed in this paper and distribution of earthquakes are shown in **Fig. 1**. The magnitudes of all selected earthquakes are more than or equal to 4.5 (Mb) and directions of their initial P motions were reported by more than six stations. The total number of selected earthquakes were 210, including three events with magnitudes of more than or equal to 6.0 and 111 events with magnitudes greater than or equal to 5.0. The range of depths of these earthquakes is from the surface to 70 km except two earthquakes. It means that earthquakes occurring in this region are shallow earthquakes in the crust. The two exceptional events, whose depths were 96.0 and 75.4 km, occurred near the Hindukush and Burma regions respectively, where intermediate

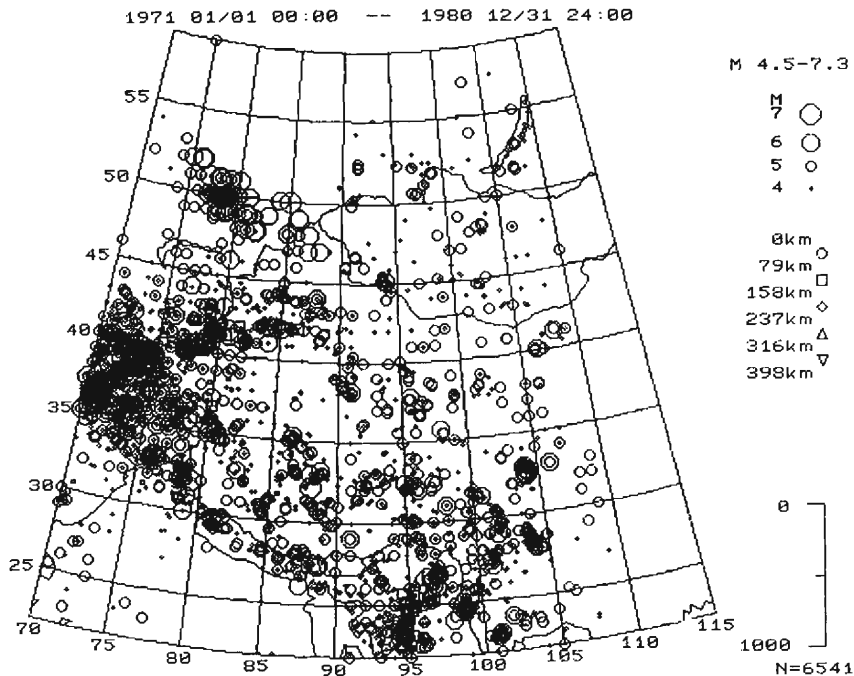


Fig. 1. Distribution of epicenters ( $M_b \geq 4.5$ ) in and around West China since 1971 to 1980 (data from B.I.S.C.).

depth earthquakes occur.

In order to obtain good solutions, two kinds of methods were used to calculate the average direction of the principal compressive axis in each region.

In one method the fault plane solution of each earthquake was obtained. Fault plane solutions of 210 events have been determined from the distribution of the polarities of initial P motions on the focal hemisphere. All results of mechanism solutions were classified into A, B and C ranks based on their reliability judging from the number and the distribution of data and the consistency of the solution. Only 99 results of A rank with high accuracy have been used to analyze the stress field in the West China region and its vicinity. These solutions are shown in **Fig. 2** and in **Table 1**.

The other method is to get averaged directions of principal axes from smoothed radiation patterns. By this method, we can determine the major directions of the principal axes of earthquakes in a restricted region, superposing distributions of the first P motions which are regarded as if they were coming from a single source. This method was developed by Aki (1966) to analyze earthquake-generating stresses in Japan.<sup>16)</sup> Oike (1971) successfully determined the world wide distribution of the earthquake-generating stresses by this method.<sup>17)</sup>

The main procedure of this method is as follows: the polarities of P motions are

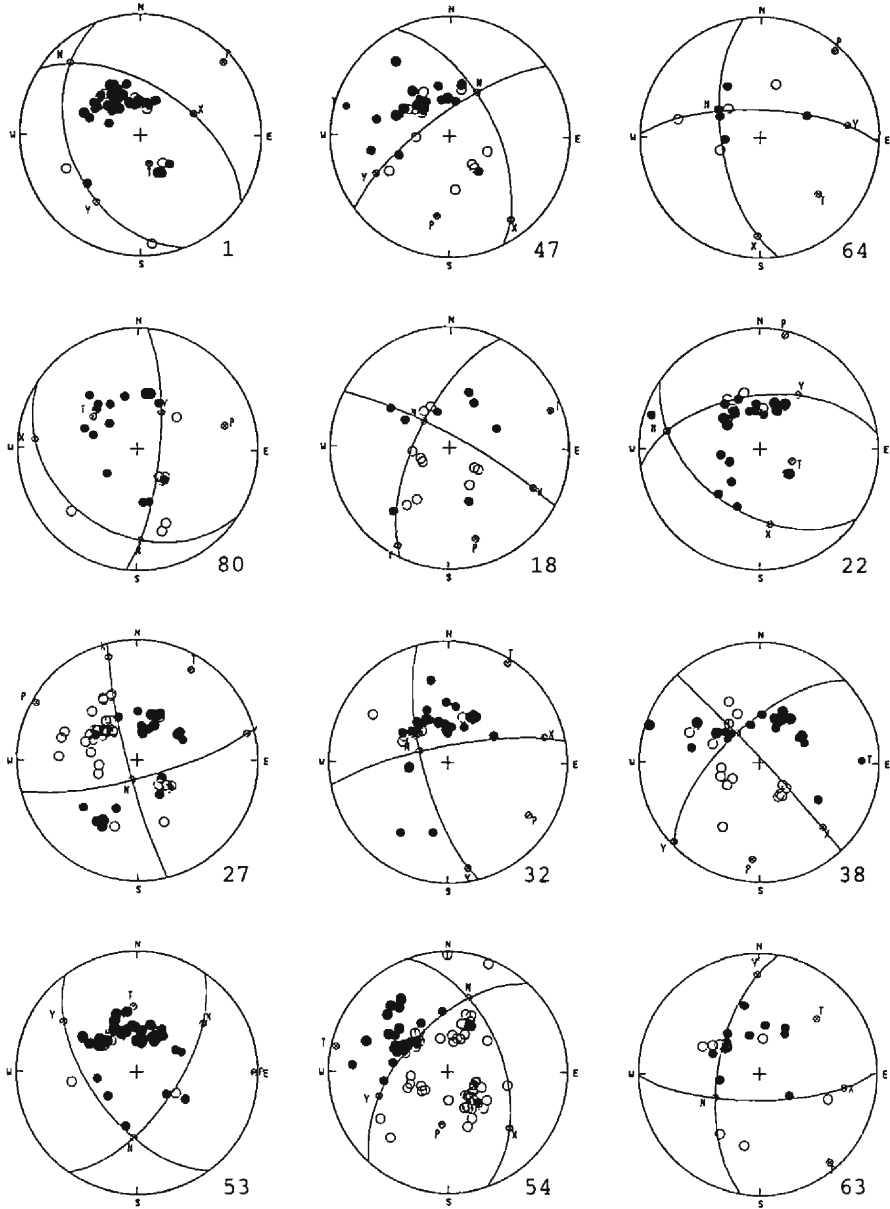


Fig. 2(a)

Fig. 2 (a)~(i). Fault plane solutions and the P wave first motion data in the form of the Wulff's net projection of lower hemisphere. Closed and open circles indicate the compressions and dilatations, respectively. The numbers correspond to those in Table I.

superposed on a focal hemisphere at first and their distribution is smoothed and normalized. The number of compressions ( $N_c$ ) and the number of dilatations ( $N_d$ )

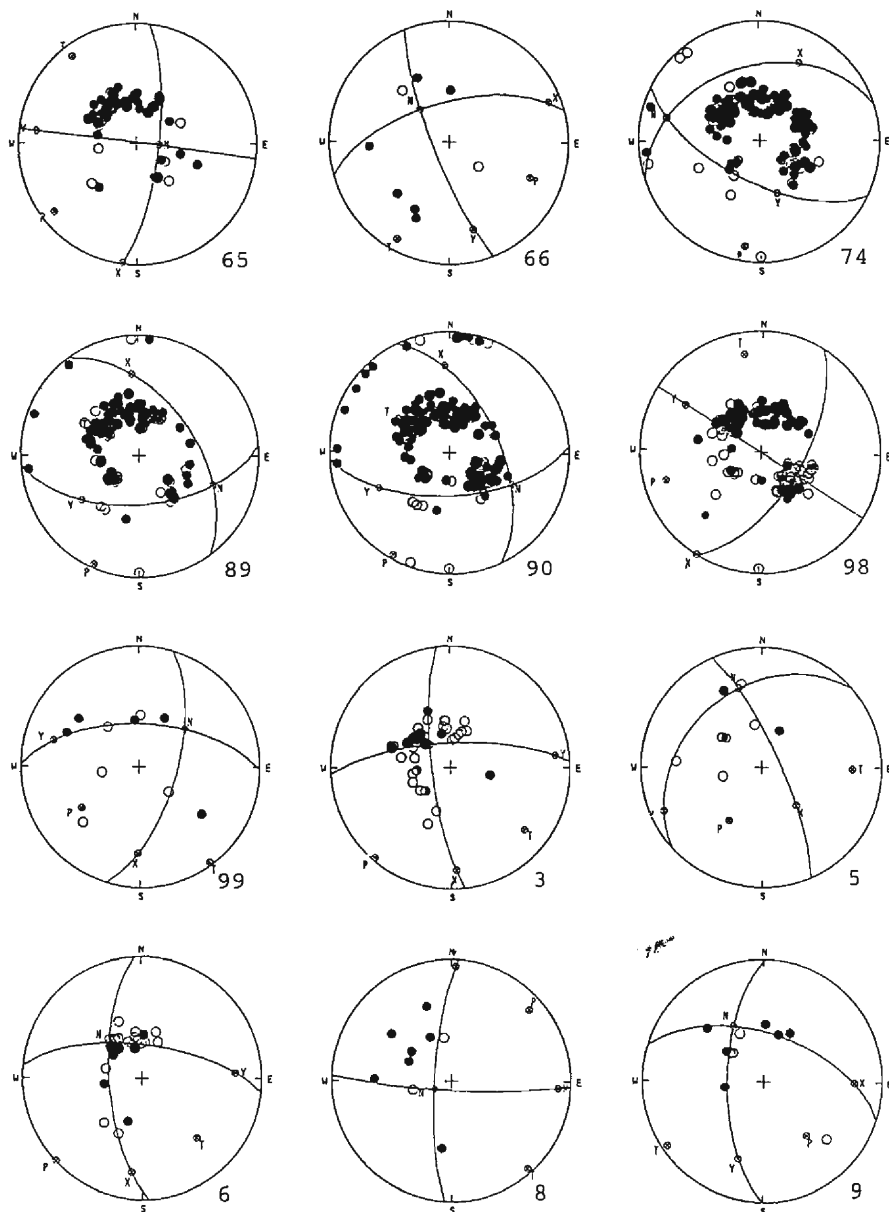


Fig. 2(b)

with in an angular distance of  $45^\circ$  from  $Q(\theta, \varphi)$  and its antipode  $Q'(\pi-\theta, \pi+\varphi)$  on a focal sphere are counted. Then a normalized parameter  $K(\theta, \varphi)$  is calculated by

$$K = (N_d - N_c) / (N_d + N_c).$$

The parameters  $K$  are calculated for 61 points of  $Q$  uniformly covering the surface of the lower hemisphere (**Fig. 4**). Then the values obtained for  $K$  are plotted on a

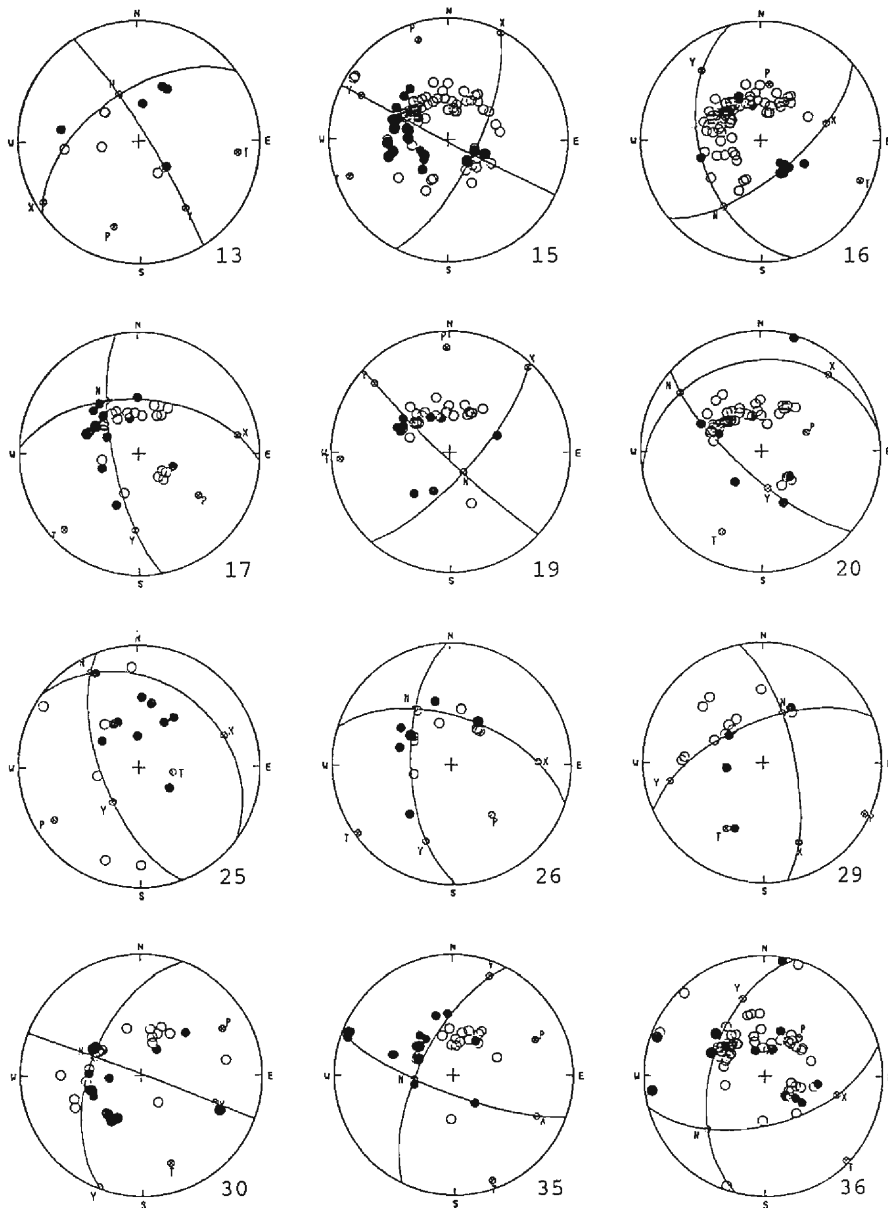


Fig. 2(c)

plane projected by Wulff's net and contour lines are drawn. The point of the maximum value of  $K$  on a focal sphere corresponds to the maximum pressure axis and that of the minimum value corresponds to the maximum tension axis.

### 3. Results of focal mechanisms in each region in and around West China

In the wide West China area, there are some different kinds of tectonic structures.

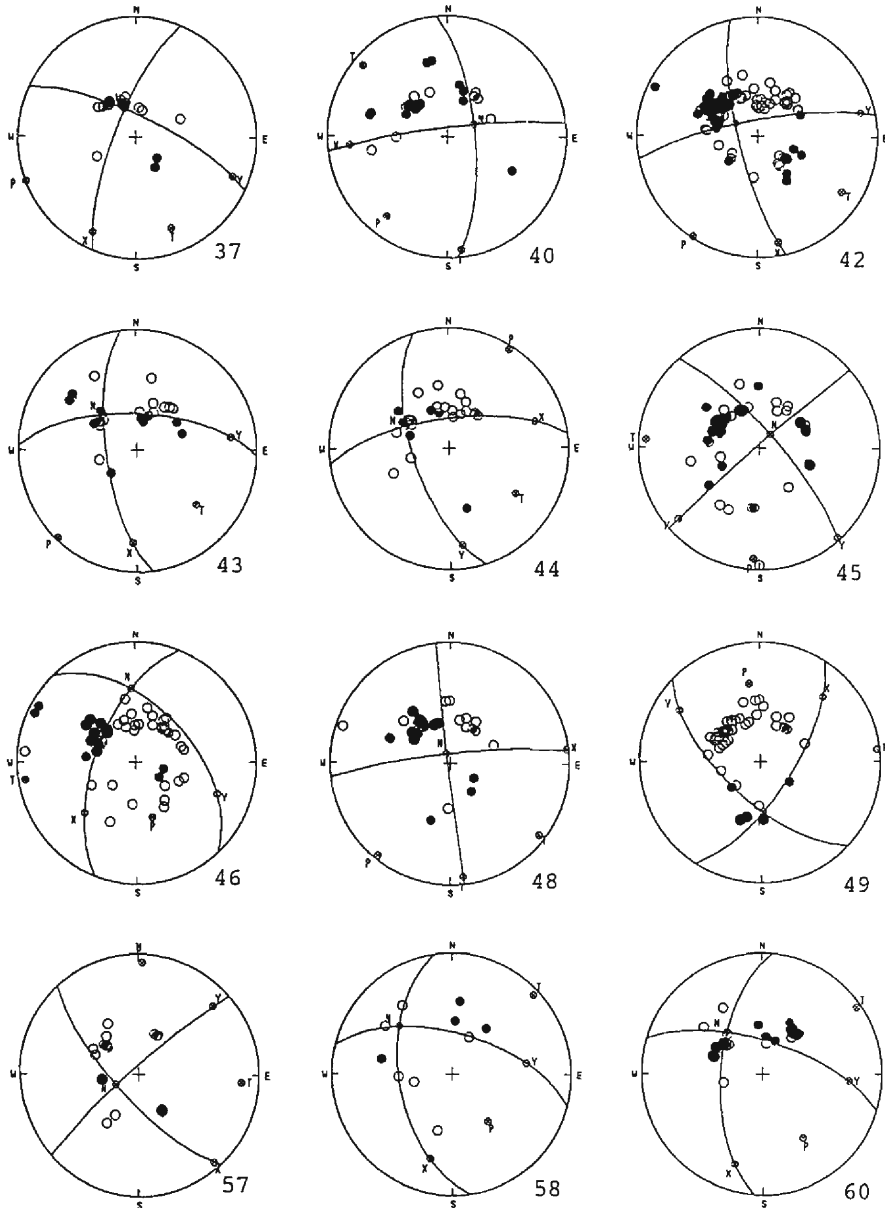


Fig. 2(d)

Therefore, there may be different characteristics of the stress fields in the various regions. In order to discuss these characteristics of the individual stress fields, we divided the wide area into three regions based on the tectonic features. They are the Himalayan mountains, the Tibetan plateau and the northwestern China regions. Moreover, each region was divided into two or three subregions, considering the



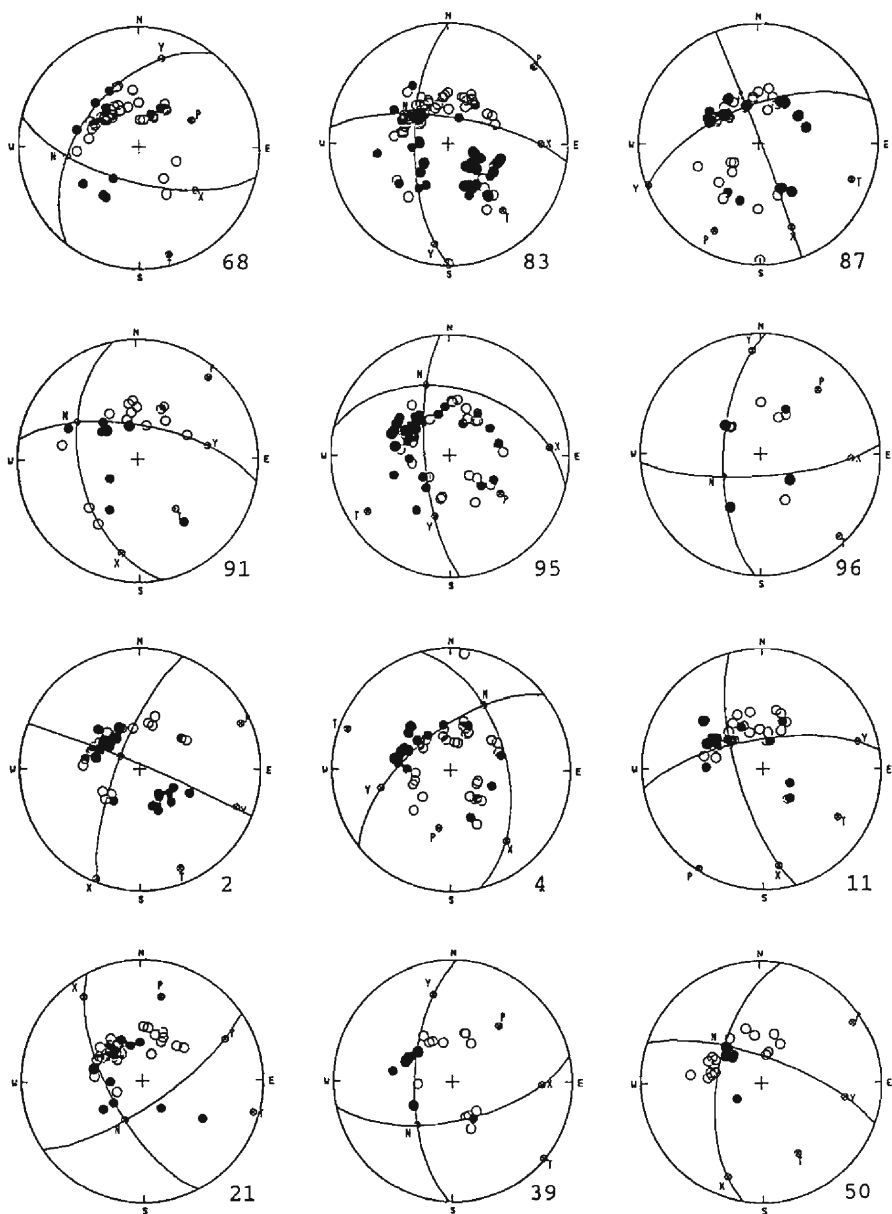


Fig. 2(e)

epicentral distribution. Therefore the whole area was divided into 8 subregions as shown in **Fig. 3**.

### 3.1. Results obtained from fault plane solutions

All results of fault plane solutions are shown in **Table 1** and **Fig. 2**. The distribution of horizontal components of P-axes and T-axes of all new mechanism

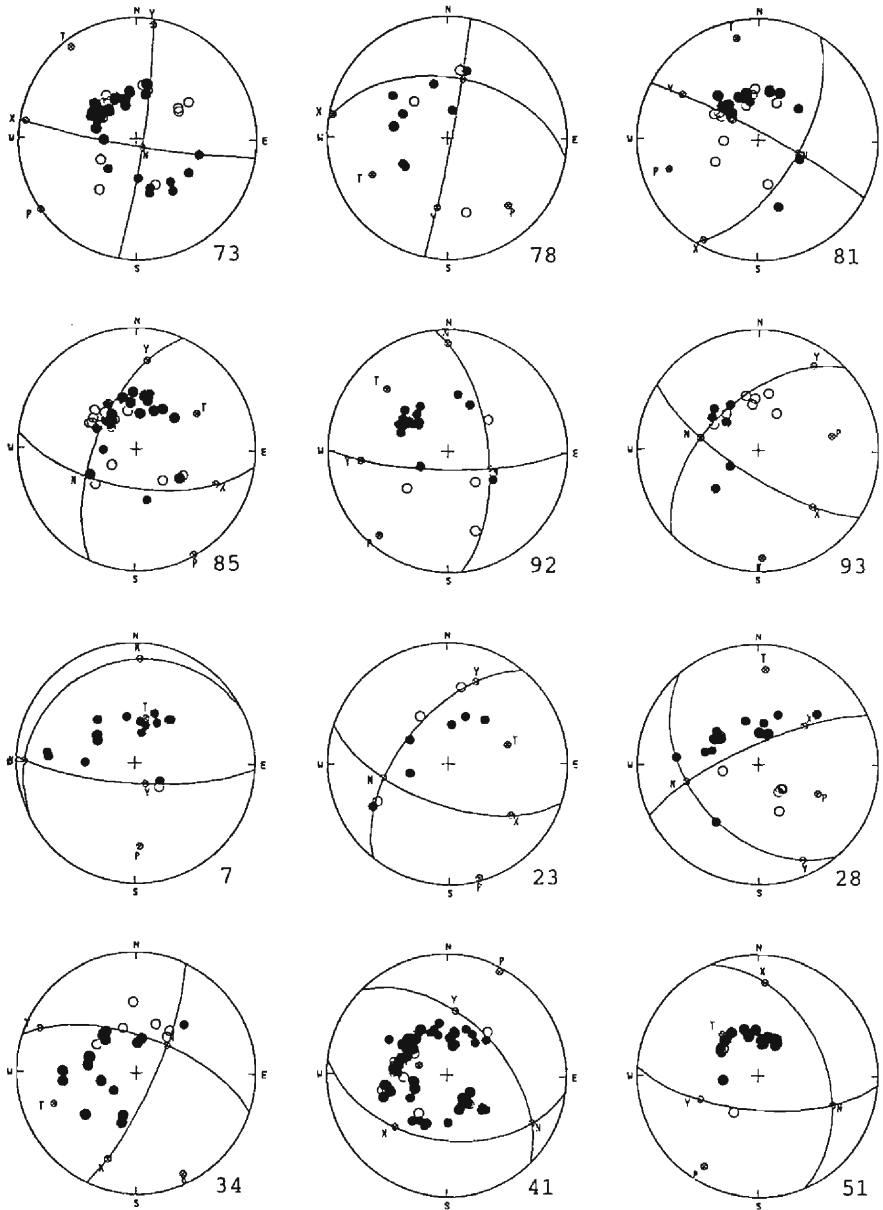


Fig. 2(f)

solutions are shown in **Fig. 5** and **Fig. 6**, respectively. The main features of the results in each region are described as follows:

### 3.1.1. The Himalayan mountain region

This region was divided into two subregions to discuss the detailed characteristics of each stress field. They are the eastern part of the Himalayas (subregion No. 1) and the central and the western part of the Himalayas (subregion No. 2).

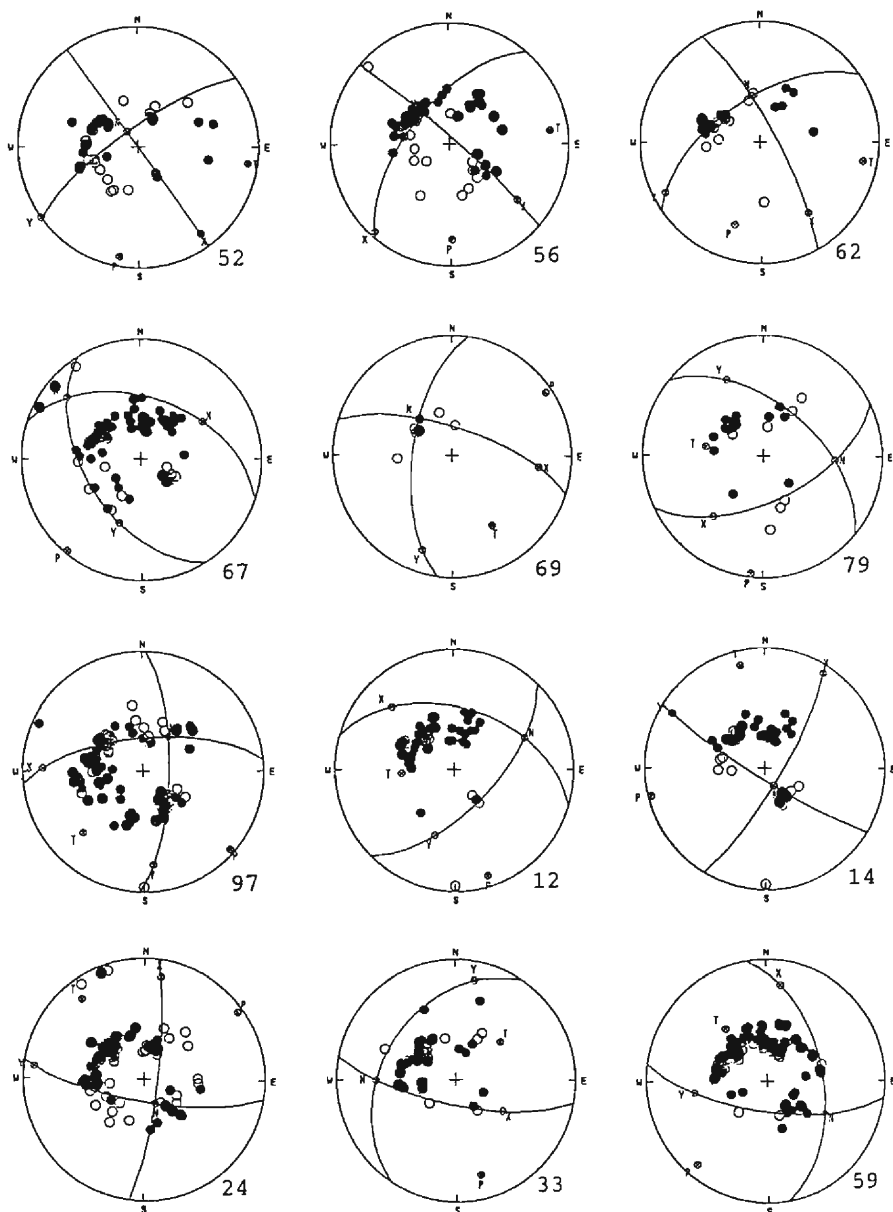


Fig. 2(g)

In the eastern part of the Himalayas, focal mechanisms of four earthquakes which occurred in the depth range from 30 to 52 km were newly determined. Two of them are reverse faulting type events and the others are strike-slip faulting type events. The P-axes lie in the NE-SW and the T-axes are in the NW-SE direction, respectively.

In the central and the western parts of the Himalayan region, many strong and

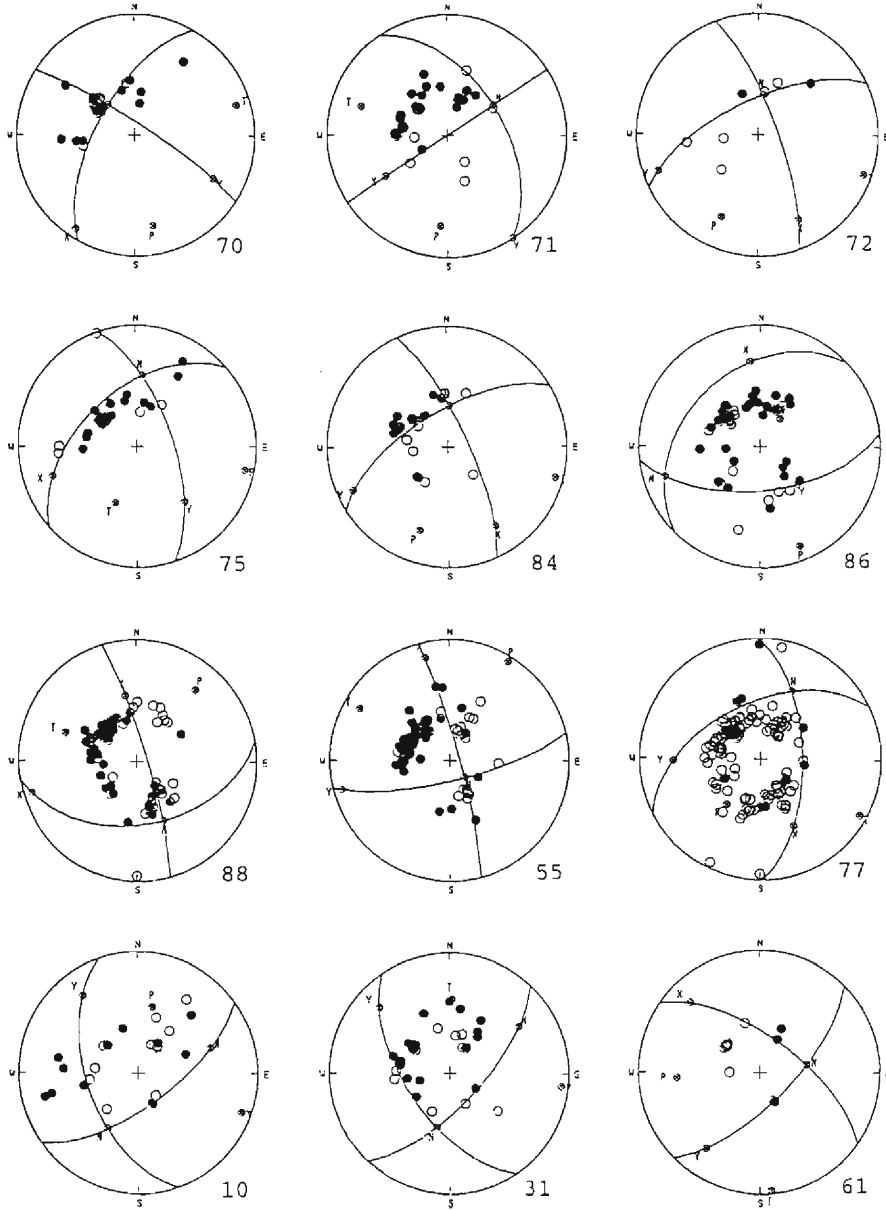


Fig. 2(h)

moderate earthquakes occurred during the 10 year period of our analyses. Fifteen solutions of earthquakes with magnitudes ranging from 4.5 to 6.1 have been obtained. Their focal depths are from 0 km to 96.0 km. It seems that shallow earthquakes occur in the central part of Himalayas and deeper earthquakes occur in the western part of this region. Although the directions of P-axes of focal mechanisms in the central and western part of the Himalayan region are a little more complicated than

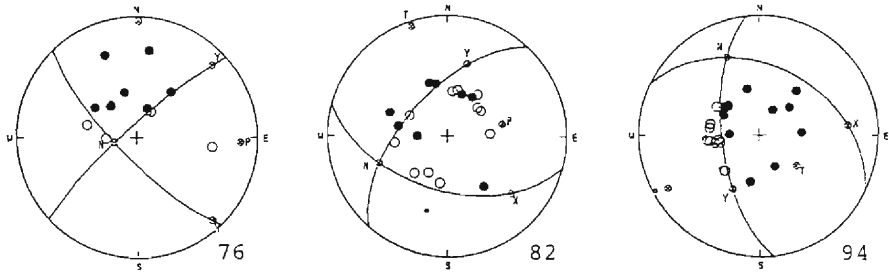


Fig. 2(i)

those in the eastern part of the Himalayan region, the major direction of P-axes are from NNE–SSW to NE–SW. T-axes are in the WNW–ESE direction. They are reverse fault types or strike-slip fault types. None of them are normal fault type.

Table 1. List of Focal Mechanisms of Events in this Paper

No.	Date			Lat. (deg)	Long. (deg)	Depth (km)	M	Reg.	P-axis		T-axis	
									Az (deg)	Pl (deg)	Az (deg)	Pl (deg)
1	Feb.	2,	1971	23.71	91.66	36	5.4	1	48	9	164	70
2	Apr.	3,	1971	32.16	94.99	0	5.6	4	66	9	158	13
3	May.	3,	1971	30.79	84.33	0	5.3	3	221	3	130	21
4	May.	22,	1971	32.36	92.11	0	5.5	4	192	50	291	7
5	Feb.	20,	1972	34.47	80.37	33	4.8	3	212	47	91	26
6	Mar.	15,	1972	30.53	84.43	0	5.1	3	227	0	137	33
7	Mar.	24,	1972	42.89	87.50	39	4.9	5	176	31	13	58
8	Apr.	21,	1972	34.99	81.15	21	4.8	3	48	13	139	4
9	Apr.	28,	1972	31.34	84.92	32	5.0	3	141	42	236	5
10	Aug.	9,	1972	52.86	107.71	33	5.0	8	13	43	110	8
11	Aug.	10,	1972	32.48	93.53	34	5.0	4	213	2	122	27
12	Aug.	30,	1972	36.56	96.35	0	5.5	6	163	9	265	54
13	Dec.	30,	1972	33.60	87.55	33	4.7	3	197	28	97	18
14	Jun.	16,	1973	37.67	95.67	0	5.3	6	256	3	347	13
15	Jul.	14,	1973	35.16	86.40	0	5.9	3	343	15	250	13
16	Jul.	14,	1973	35.21	86.54	0	5.7	3	8	51	112	11
17	Jul.	16,	1973	35.03	86.50	0	5.2	3	124	40	225	13
18	Aug.	1,	1973	29.59	89.17	63	4.9	2	163	23	69	10
19	Aug.	16,	1973	33.24	86.84	0	5.3	3	359	14	267	8
20	Sep.	8,	1973	33.29	86.82	11	5.5	3	67	57	207	27
21	Sep.	9,	1973	31.61	99.99	21	5.5	4	13	29	106	5
22	Oct.	16,	1973	28.36	82.99	0	5.0	2	13	4	111	67
23	Nov.	28,	1973	37.88	81.52	33	4.9	5	165	3	72	46
24	Jul.	4,	1974	45.20	93.86	0	5.9	6	53	4	322	17
25	Jul.	7,	1974	30.55	78.48	96	4.7	3	239	18	99	67
26	Aug.	3,	1974	35.68	80.65	0	4.7	3	141	46	235	3
27	Sep.	27,	1974	28.59	85.51	20	5.5	2	300	4	31	13
28	Sep.	30,	1974	43.09	88.48	26	4.9	5	116	44	4	21
29	Oct.	13,	1974	34.76	87.23	33	5.1	3	116	4	210	37
30	Nov.	29,	1974	51.77	98.73	28	5.2	3	60	23	162	25
31	Dec.	18,	1974	48.35	103.29	0	5.0	8	96	6	2	38

Table 1. List of Focal Mechanisms of Events in this Paper

No.	Date			Lat. (deg)	Long. (deg)	Depth (km)	M	Reg.	P-axis		T-axis	
									Az (deg)	Pl (deg)	Az (deg)	Pl (deg)
32	Dec.	23,	1974	29.32	81.38	45	5.2	2	123	21	31	4
33	Jan.	4,	1975	38.58	97.46	33	5.3	6	165	21	50	49
34	Jan.	14,	1975	43.67	86.88	12	4.9	5	155	9	249	27
35	Jan.	19,	1975	32.30	78.66	0	5.1	3	67	26	160	7
36	Jan.	19,	1975	32.39	78.50	1	6.2	3	42	54	135	2
37	Jan.	19,	1975	31.94	78.52	49	5.8	3	248	0	158	21
38	Jan.	31,	1975	28.09	84.77	19	5.0	2	184	20	88	16
39	Feb.	1,	1975	32.56	93.61	7	4.7	4	40	39	129	1
40	Feb.	2,	1975	32.55	78.50	21	5.1	3	217	18	310	9
41	Mar.	31,	1975	46.66	91.31	6	5.2	5	27	3	288	70
42	Apr.	28,	1975	35.80	79.86	0	5.8	3	213	1	123	18
43	Apr.	28,	1975	35.95	79.97	31	5.2	3	223	2	132	34
44	Apr.	29,	1975	35.83	79.88	0	5.0	3	32	3	124	33
45	May.	19,	1975	35.12	80.84	6	5.5	3	183	10	274	7
46	Jun.	4,	1975	35.83	79.92	0	5.6	3	163	51	261	6
47	Jun.	10,	1975	28.19	95.91	30	4.9	1	189	34	286	10
48	Jul.	19,	1975	31.95	78.59	0	5.1	3	218	4	128	6
49	Jul.	29,	1975	32.57	78.49	0	5.5	3	352	34	84	3
50	Nov.	7,	1975	33.29	95.31	27	5.1	4	58	8	154	35
51	Mar.	20,	1976	41.76	88.67	8	5.0	5	211	14	319	53
52	Apr.	1,	1976	51.16	97.99	8	5.2	5	190	9	99	9
53	May.	10,	1976	29.33	81.46	0	5.2	2	90	3	357	45
54	Sep.	14,	1976	29.81	89.57	75	5.4	2	187	54	283	4
55	Sep.	22,	1976	40.06	106.33	18	5.5	7	31	5	300	15
56	Jan.	1,	1977	38.19	90.97	0	5.8	5	179	23	82	16
57	Jan.	6,	1977	31.25	87.98	0	5.5	3	2	8	94	15
58	Jan.	14,	1977	34.68	82.83	33	4.7	3	142	49	46	5
59	Jan.	19,	1977	37.02	95.73	0	5.8	6	221	11	322	44
60	Feb.	19,	1977	34.63	81.29	19	5.1	3	148	37	55	4
61	Sep.	10,	1977	57.29	106.24	33	4.8	8	266	32	175	3
62	Oct.	19,	1977	39.15	91.04	0	5.2	5	198	29	101	13
63	Nov.	4,	1977	29.50	81.30	17	4.8	2	141	7	47	33
64	Nov.	13,	1977	26.51	93.00	52	5.1	1	40	5	133	34
65	Feb.	10,	1978	28.03	84.70	0	5.3	2	231	12	323	10
66	Feb.	19,	1978	29.30	84.97	22	4.5	2	113	27	209	11
67	Apr.	22,	1978	41.96	85.87	0	5.3	5	220	2	124	69
68	Aug.	8,	1978	32.27	83.10	3	5.1	3	63	49	164	10
69	Oct.	14,	1978	41.42	88.66	33	4.9	5	56	5	150	34
70	Oct.	16,	1978	45.15	93.75	37	5.1	6	169	24	73	12
71	Nov.	17,	1978	37.25	97.07	15	5.0	6	185	26	289	26
72	Feb.	12,	1979	44.94	94.13	13	4.7	6	204	27	110	7
73	Mar.	29,	1979	32.44	97.26	0	5.4	4	234	0	324	7
74	May.	20,	1979	29.93	80.27	0	5.7	2	189	13	70	64
75	Jun.	25,	1979	45.24	98.70	52	5.0	6	102	8	202	49
76	Jul.	11,	1979	48.00	103.26	30	4.8	8	93	15	2	4
77	Aug.	24,	1979	41.16	108.13	0	5.7	7	216	51	119	6
78	Aug.	26,	1979	32.84	95.38	25	4.7	4	137	26	244	30
79	Sep.	28,	1979	38.22	90.44	19	5.0	5	186	3	279	50

Table 1. List of Focal Mechanisms of Events in this Paper

No.	Date			Lat. (deg)	Long. (deg)	Depth (km)	M	Reg.	P-axis		T-axis	
									Az (deg)	Pl (deg)	Az (deg)	Pl (deg)
80	Sep.	29,	1979	29.04	95.80	35	5.0	1	74	25	306	53
81	Dec.	6,	1979	30.05	95.48	12	5.2	4	251	24	348	15
82	Feb.	6,	1980	51.76	105.46	3	4.8	8	78	51	342	5
83	Feb.	22,	1980	30.55	88.65	14	5.7	3	48	3	140	30
84	Mar.	6,	1980	36.12	91.95	0	5.0	6	200	28	106	7
85	Apr.	13,	1980	30.20	95.52	30	5.1	4	150	1	59	40
86	Jun.	1,	1980	38.91	95.60	50	5.2	6	158	13	36	67
87	Jun.	24,	1980	33.00	88.55	3	5.1	3	208	20	111	17
88	Jul.	12,	1980	36.88	93.77	0	5.4	6	40	24	292	36
89	Jul.	29,	1980	29.34	81.21	3	5.7	2	203	4	299	56
90	Jul.	29,	1980	29.63	81.09	0	6.1	2	209	4	303	48
91	Aug.	14,	1980	32.99	88.57	33	4.9	3	41	10	143	48
92	Aug.	23,	1980	30.35	94.89	34	4.7	4	219	10	315	28
93	Sep.	9,	1980	30.27	94.93	41	4.6	4	78	38	178	12
94	Oct.	2,	1980	51.35	107.28	0	5.0	8	240	13	129	57
95	Oct.	7,	1980	35.62	82.14	0	5.4	3	127	47	237	18
96	Oct.	8,	1980	31.43	87.72	34	5.0	3	42	29	136	7
97	Nov.	6,	1980	43.75	86.20	7	5.5	5	132	3	224	29
98	Nov.	19,	1980	27.40	88.80	1	6.0	2	252	19	350	19
99	Nov.	20,	1980	29.52	85.23	37	4.8	2	235	41	143	2

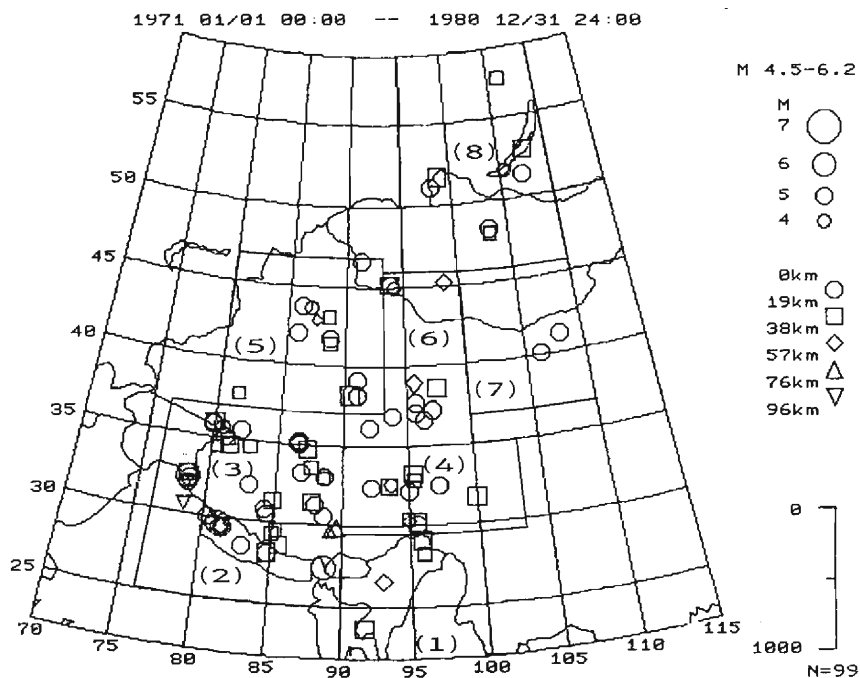


Fig. 3. Division of subregions and distribution of epicenters analyzed in this paper.

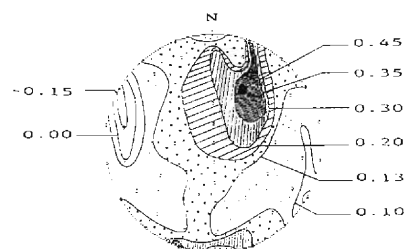


Fig. 4. An example of the smoothed radiation pattern indicated by the equal lines of K value. The maximum value of K and the minimum one of K corresponds to maximum pressure and tension, respectively.

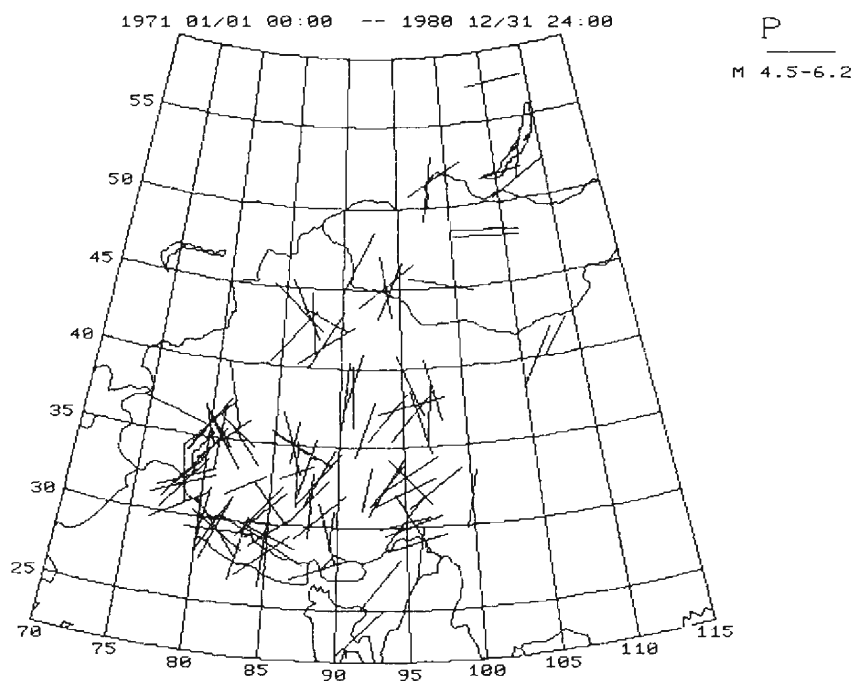


Fig. 5. Distribution of compressional axes obtained in this paper.

The mechanism solution of the largest earthquake ( $M=6.1$ , July 29, 1980,  $29.63^{\circ}\text{N}$ ,  $81.09^{\circ}\text{E}$ ,  $h=0$  km) in this region was reverse fault type. It shows that the major characteristics of the stress field in the Himalayan region are compressive stresses in the NNE–SSW direction.

### 3.1.2. The Tibetan plateau region

This wide region includes the western and the central part (subregion No. 3) and the eastern part of Tibet (subregion No. 4).

Many large earthquakes have occurred during the past 10 years in the western



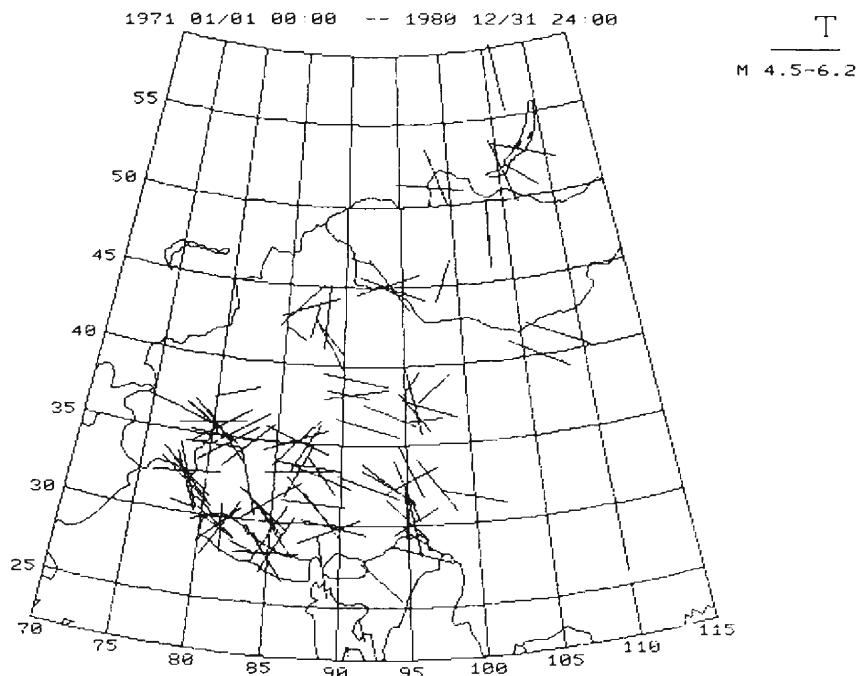


Fig. 6. Distribution of extensional axes obtained in this paper.

part of this region. Among these fault plane solutions of 17 shallow events were obtained. They show that the P-axes are mainly in the N-S to NE-SW directions and the T-axes are in the E-W to NW-SE directions in this region, except for a few events with P-axes in the NW-SE direction. However the most notable feature is that almost all of the fault plane solutions among the 17 events have normal or strike slip faults with large normal faulting components.

The largest event ( $M=6.2$ , January 19, 1975,  $32.39^{\circ}\text{N}$   $78.50^{\circ}\text{E}$ ,  $h=1$  km) in this region exhibited normal faulting mechanism with T-axes approximately in the SE-NW direction and P-axes approximately in the NE-SW direction. No thrust faulting occurred in this region. The major characteristics of earthquake mechanisms in this region are very different from those of the Himalayan region.

We also determined fault plane solutions of 18 events ( $M>4.6$ ) in the central part of the Tibetan region where the seismic activity is high. All solutions showed strike-slip or normal faulting except one with thrust fault. Most of these P-axes lie in the N-S to NE-SW directions and T-axes lie in the E-W to SE-NW directions. A few fault plane solutions among those on the boundary between Tibetan plateau and the Xingjiang regions show the P-axes with NW-SE direction and T-axes with NE-SW direction.

The eastern part of the Tibetan region, which is the southern part of the North-South Seismic Belt, is one of the most active regions in China. Focal mechanism

solutions of 12 earthquakes in this region from those occurring during the past 10 years have been analyzed. Most of them showed left-lateral strike-slip faults while a few of them showed normal faults. Their P-axes are in between the NNE–SSW and the ENE–WSW directions, except that the P-axes of a few events with magnitudes less than 5.1 are in the NW–SE direction which seems to be related to the stress field of the eastern part of China.

### **3.1.3. The northwestern China region and other regions**

The northwestern China region is divided into two subregions: Xingjiang (subregion No. 5) and a part of Qilian mountains (subregion No. 6). There are many famous seismic zones, for example the Tianshan Seismic Belt, the Qilianshan Seismic Belt and so on.

In the Xingjiang region of China, focal mechanism solutions of 13 earthquakes from 1971 to 1980 were obtained. All of them show either reverse faulting or strike-slip faulting, and none of them show normal faulting. The P-axes of almost all of the 13 are in the N–S to NNE–SSW directions. Only three of them in eastern Tianshan have P-axes in the NW–SE direction. It seems that the direction of P-axes in this region are related to compressive forces from the Tibetan plateau region.

In the Qilian mountains region, which is the northern border of the Tibetan plateau, many historical strong earthquakes have occurred. However some moderate events occurred here from 1971 to 1980. Solutions of focal mechanisms of 12 earthquakes show that they were caused by strike-slip faults and thrust faults. The P-axes from these solutions are mainly in the N–S to NNE–SSW directions. The orientations of the T-axes are nearly in the E–W direction.

In the northwestern side of Ordos (subregion No. 7), only two moderate earthquakes occurred from 1971 to 1980. One of them is the Bayenmuren earthquake of magnitude 5.5 on September 22, 1976. Its focal mechanism shows that this was caused by a right-lateral fault and the azimuths of the P-axis and the T-axis were  $31^\circ$  and  $300^\circ$ , respectively. The other is the Wuyuan earthquake of magnitude 5.7 on August 24, 1979. The fault plane solution of this event indicates that it was a normal fault type event and the azimuths of P-axis and T-axis were  $216^\circ$  and the  $119^\circ$ , respectively.

In the northern region (subregion No. 8), including a part of Mongolian and Baikal lake region, P-axes lie almost in the NNE–SSW to E–W directions and T-axes lie in the WNW–ESE to N–S directions.

## **3.2. Results obtained from smoothed radiation patterns**

In order to add more information from other events, averaged orientations of P-axes and T-axes of the stress field were determined from smoothed radiation patterns. These were obtained mainly from data of B and C rank events from 1971 to 1980. In some regions where the quantity of data for the B and C rank events were not enough to procure reliable results, all the data available was used. The distribution of B and C rank events and the regions analyzed are shown in **Fig. 7**. The results

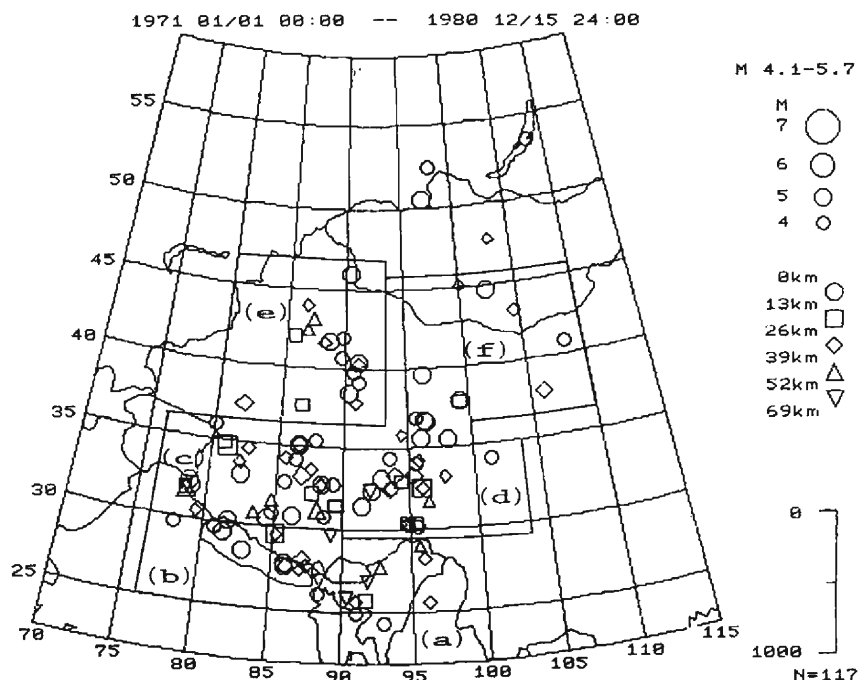


Fig. 7. Distribution of epicenters of the events with the accuracies of B and C rank and the division of subregions.

Table 2. List of regional data and results. Regional number correspond to those in Fig. 7. The Ne, Nc and Nd correspond to the total number of earthquakes, the total number of compressions and the total number of dilatations, respectively.

No	Region		Ne	Nc	Nd	P axis			T axis			Rank
	Lat.(N) (deg)	Long.(E) (deg)				max. k	$\phi$ (deg)	$\theta$ (deg)	min. k	$\phi$ (deg)	$\theta$ (deg)	
a	22-29.5	90-100	11	78	43	1.00	180	80	-1.00	350	85	A
b	25-30	76-90	12	152	83	0.60	230	80	-1.00	80	85	A
c	30-37	76-90	64	873	1264	0.43	30	60	-0.14	290	85	A
d	29.5-35	90-103	31	432	379	1.00	80	90	-0.38	340	80	A
e	37-47	80-93	28	557	282	0.5	0	90	-0.55	240	80	A
f	35-46	93-110	23	632	388	1.00	240	90	-1.00	260	90	B
	35-37	90-93										

obtained by this method are shown in **Table 2** and in **Fig. 8**.

### 3.2.1. The Himalayan mountain region

The Himalayan region was divided into two parts: the eastern part (subregion No. a) and the central and western part (subregion No. b).

The smoothed radiation pattern in the eastern part of the Himalayan region is shown in **Fig. 8(a)**. This solution shows that the maximum pressure axis corresponding to the maximum K value is in the N-S direction and the minimum pressure axis corresponding to the minimum K value is in the NNW-SSE direction. It agrees

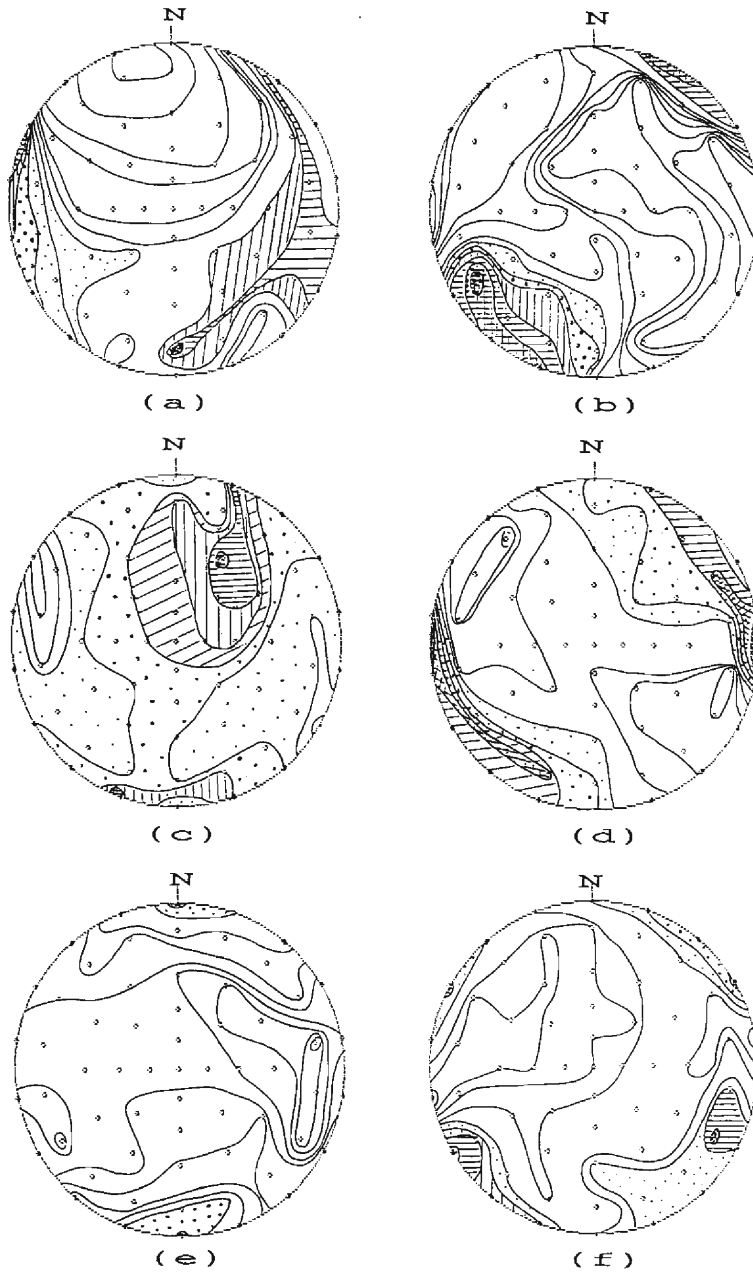


Fig. 8. Smoothed radiation patterns for subregions.

- (a) The eastern part of the Himalayan region
- (b) The central and western part of the Himalayan region
- (c) The western and central part of the Tibetan plateau
- (d) The eastern part of the Tibetan plateau
- (e) The Xingjiang region
- (f) The Qilianshan region and the northwestern side of Ordos.

well with the solutions from polarities of initial P motions and reveals strike-slip faulting with a large reverse component.

The smoothed radiation pattern of the central and the western part of the Himalayan region shown in **Fig. 8(b)** indicates that the orientations of the P-axis and T-axis are in the NE–SW and E–W directions, respectively. The orientation of the P-axis of a smoothed radiation pattern with the reverse faulting component is nearly perpendicular to the trend of the Himalayan mountain arc. The natural conditions are also similar to those from the solutions obtained by data of initial P motions in this region.

### 3.2.2. The Tibetan plateau region

This region includes subregion No. c and subregion No. d. The smoothed radiation pattern in the western and central part of Tibet region is shown in **Fig. 8(c)**. It can be seen that the orientations of P-axis and T-axis in this region are in the NNE–SSW and WNW–ESE directions, respectively. And it seems that the extensional stress in the WNW–ESE direction prevails in this region. The natural conditions are again similar to that from the solutions of focal mechanisms as mentioned in the former section.

In the eastern part of the Tibetan plateau, the result of the smoothed radiation pattern (**Fig. 8(d)**) indicates that the axis of the maximum pressure is nearly in the

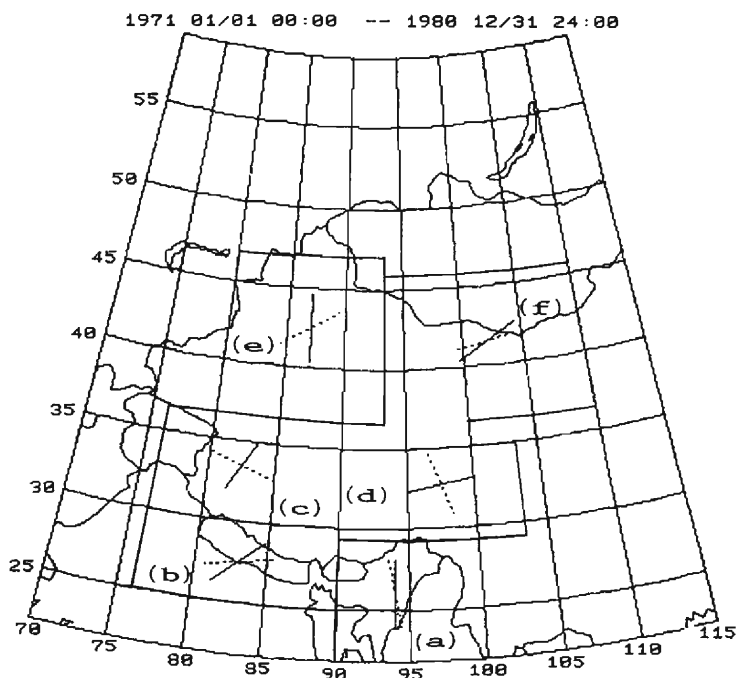


Fig. 9. The orientations of the P-axes and the T-axes in six subregions obtained from smoothed radiation patterns.

ENE–WSW direction and that of the minimum pressure is in the NW–SE direction. Active faults with the strike-slip movements predominate in this region.

### **3.2.3. The northwestern China region and other regions**

The result of smoothed radiation pattern in the Xingjiang region is shown in **Fig. 8(e)**. The  $K$  values of almost all points are less than 0, except a few points located around the northern and southern ends. The orientation of P-axis and T-axis are in the N–S and E–W directions, respectively.

The **Fig. 8(f)** shows the result of smoothed radiation pattern in the Qilianshan region and the northwestern side of Ordos. It seems that the orientation of the T-axis is nearly in the E–W direction and the orientation of the P-axis is in the NE–SW direction. This result does not conform as well as those in other regions. This implies that the stress field in this region is not as simple as those in the Himalayan and Tibet regions.

All results obtained from smoothed radiation patterns in the six regions are shown in **Fig. 9**. The results of B and C rank events are consistent with the results obtained from the initial P motion data of A rank events.

## **4. Characteristics of the tectonic stress in West China**

Results obtained in this study are shown in **Figs. 5, 6, 8 and 9**. The distributions of P-axes and T-axes of fault plane solutions of earthquakes from 1971 to 1980 compiled by Ishikawa (1988) are shown in **Fig. 10**.<sup>18)</sup> The total number of events in **Fig. 10** is 75, and they are concentrated in the surrounding regions of the area analyzed in this paper. Almost all of them are different events from those newly analyzed in this study. The orientations of P-axes and T-axes shown in **Fig. 10** are consistent with the results in **Figs. 5 and 6**. From all of these results, the characteristics of the stress field in West China are summarized as follows.

The active tectonics in the Himalayan region are characterized by the compressive stress in the NNE–SSW to NE–SW directions. The orientations of P-axes are almost perpendicular to the Himalayan arc in all sections, with the orientations of T-axes being along this arc.

In the Tibetan region, most of the fault plane solutions of events in the higher plateau (in the region of 31°N–36°N, and 78°E–87°E) show that they occur by normal or the combination of normal and strike-slip faults. Moreover, the result obtained from the smoothed radiation pattern also shows that they have a large normal component. This suggests that the extensional stress field with T-axes nearly in the E–W or WNW–ESE directions dominates the seismo-tectonics in the higher Tibetan region and P-axes in the N–S to NE–SW directions in this region do not play an important role in the tectonics.

Thrust type faulting is clearly predominant in the boundary regions around the Tibetan plateau, except in the eastern boundary. The orientations of the P-axes are mainly in the N–S or NE–SW directions, except a few events with P-axes in the NW–

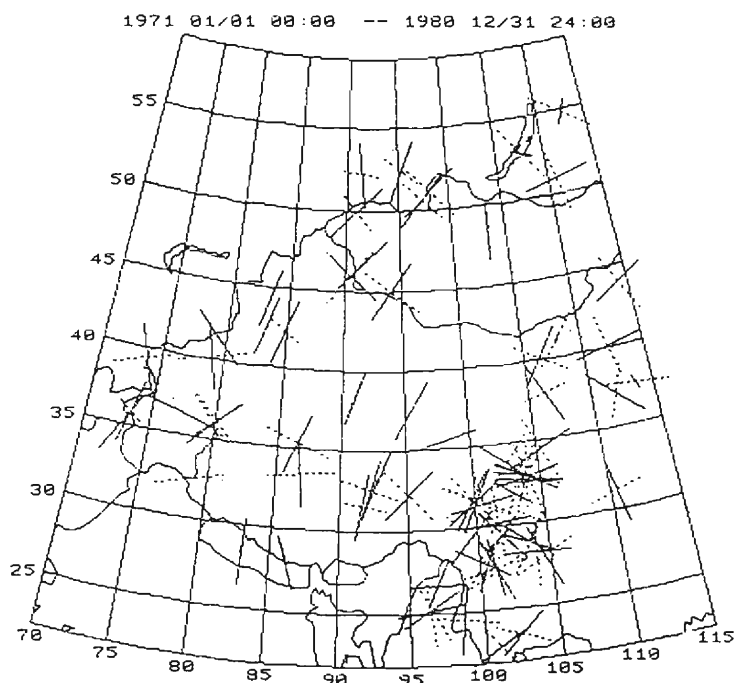


Fig. 10. Distributions of compressional axes (solid lines) and extensional axes (dotted lines) in and around West China (after Ishikawa,<sup>18)</sup>).

SE direction. On the eastern boundary of the Tibetan plateau, a lot of events are caused by strike-slip faults. The characteristics of the tectonic stress field in the higher Tibetan plateau are different from those in its surrounding regions.

In the northwestern region, the most noticeable characteristics of the stress field are that all results show reverse faulting or strike-slip faulting and the compressional forces in the direction from nearly N-S to NE-SW dominate the earthquake-generating stresses in this region. It indicates that this wide area is compressed by neighboring crustal blocks. In the northern margins of the Chaidamu Basin and the Tarim Basin, the P-axes of solutions are in the NW-SE direction and T-axes are in the E-W direction.

The distributions of normal fault types, the thrust fault type and strike-slip type events in West China from all the results of fault plane solutions are shown in **Fig. 11**. This clearly indicates the distribution of the compressive and extensional characteristics in the active tectonics in this area.

## 5. Discussion and conclusion

Concerning the stress field in West China, Yan et al. (1979) suggested that the compressive activity in the N-S to NE-SW directions exists in the main part of the

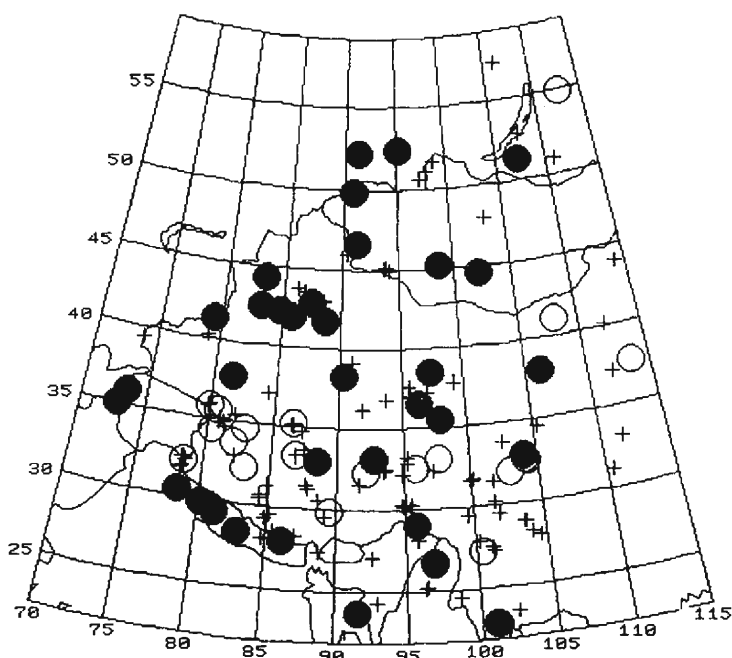


Fig. 11. Distributions of the events with the fault plane solution analyzed in this paper: open circles, closed circles and crosses correspond to the normal fault type, the reverse fault type and strike-slip fault type events, respectively.

Tibetan Plateau region extending to the west Mongolia region, and the compressive stress change in the NW-SE direction in the west Tianshan Mountains region.<sup>15)</sup> Otsuki (1985)<sup>19)</sup> compiled various data from many results and drew up a map of the horizontal projection of trajectories of principal stress axes. His main results in this region are consistent with the result by Yan et al. (1979). From the interpretation of LANDSAT image data of the Tibetan region and fault plane solutions of 14 earthquakes in the central part of the Tibetan plateau region, Molnar et al. (1978) suggested that the active tectonics of this region are dominated by extension in the E-W direction.<sup>20)</sup> This result is opposes the view points of the results mentioned above. Ni and York (1978) also pointed out that there was a Late Cenozoic east-west extension in the Tibetan plateau.<sup>21)</sup>

More than two hundreds focal mechanisms of large and moderate crustal earthquakes in the region from the Himalayan mountains to Lake Baikal have been newly obtained and presented in this paper. Two clear characteristics of the stress field in this area can be conclusively stated. The first is that almost the orientations of P-axes of the focal mechanisms are nearly in the NNE-SSW and in the N-S directions except a few events along margins of some subregions. The second is that the major fault plane solutions in the higher Tibetan plateau have a normal component, and this fact is revealed by the occurrence of normal faulting. These events are located in the



region from the Gangdise mountains in the south to the Kunlun mountains in the north, and from the east end of the Karakorum mountains in the west to the southern part of the North-South Seismic Belt. But in the other regions of West China, almost all fault plane solutions show reverse faulting or strike-slip faulting with large thrust components.

Several models for the evolution of the Himalayan mountains and Tibetan plateau and seismo-tectonics in this area have been presented. Dewey and Bird (1970) suggested the underthrusting of the Indian plate beneath the Eurasian landmass during the Miocene and the Pliocene periods.<sup>23)</sup> Minster et al. (1974) and Tapponnier and Molnar (1977) suggested that the Indian plate is moving toward the Eurasian plate, and collision between them occurred 30 Ma ago.<sup>24,5)</sup> Both of these hypotheses are supported by our results of the orientations of the P-axes from fault plane solutions in this region. The results show that the tectonic forces from the collision between these plates cause a wide distribution of P-axes in the same direction as the relative movement between them.

Zhao et al. (1988)<sup>10)</sup> analyzed the regional characteristics of seismicity in West China and its vicinities. Their results suggest that the seismicity of the Hindukush, the Tibetan plateau, Xingjiang, the northern part and the southern part of the North-South Seismic Belt present synchronous variations, which were high around 1910, 1930's, 1950 and 1970's. The active and quiet periods in the temporal variations of the seismicity in these regions correlated with each other. This kind of characteristic temporal variation in seismic activity in West China and its vicinity also imply that the earthquake generating stress field in these regions are formed under common tectonic conditions. There is the transmission of tectonic force from the collision between the Indian and Eurasian plates along the Himalayan mountains.

Concerning other factors, many microplates lie between the Eurasian and Indian plates.<sup>11)</sup> They may contribute to the eastward deviation of tectonic forces in this region caused by the northward movement of Indian plate. This may be related to the complex distribution of P-axes along the boundaries of the microplates.

Khatttri (1987) suggested that the Tibetan plateau underthrusts from beneath the Himalayan mountains in the Indus-Tsangpo Suture fault lying along the southern side of the Tibetan plateau.<sup>9)</sup> His suggestion indicating that extensional faulting exists in the Tibetan plateau is also supported by the results obtained in this study.

The weight of a high plateau and the buoyancy acting on the bottom of the crust from the mantle may create an additional vertical compressive stress ( $\sigma_{zz}$ ). This effect may overcome the horizontal compressive stress ( $\sigma_{xx}$ ) and cause normal fault type events. Froidevaux and Ricard (1987)<sup>25)</sup> proposed an idea that the evolution of the Tibetan plateau may be considered as occurring in three stages. In the first stage, the structure was build-up by thrusting and folding under the average vertical stress ( $\sigma_{zz}$ ) which was less than the minimum principal average horizontal stress ( $\sigma_{hmin}$ ) and the maximum one ( $\sigma_{hmax}$ ). In the second stage, the neutral states or strike-slip deformations occurred under the ( $\sigma_{zz}$ ) greater than ( $\sigma_{hmin}$ ) and less than

( $\sigma_{hmax}$ ). In the third stage, ( $\sigma_{hmax}$ ) weakened and become less than ( $\sigma_{zz}$ ). This resulted in the relaxation of the topography and corresponding thinning of the crust with normal faultings. The high Tibetan plateau is now in the third stage of its history. The average altitude of this region of Tibetan plateau is more than 5000 meters (**Fig. 12**). Normal fault type events occur there. The horizontal compressive forces act in the lower places surrounding the high plateau. Therefore, almost all of fault plane solutions are thrust fault type in the low regions, namely the southern margin of the Himalayan mountains and in the northern margin of the Qilian mountains. This hypothesis seems to explain the occurrences of normal faults by extensional stresses in the E-W direction in the Tibetan region.

From the fault plane solutions in **Fig. 2**, it can be seen that strikes of one plane of the normal fault type events in high Tibetan plateau were roughly in the N-S direction. **Fig. 13** (after Molnar et al. 1978) shows the distribution of extensional



Fig. 12. Contour map in the western part of China. The numbers show altitudes in meters.

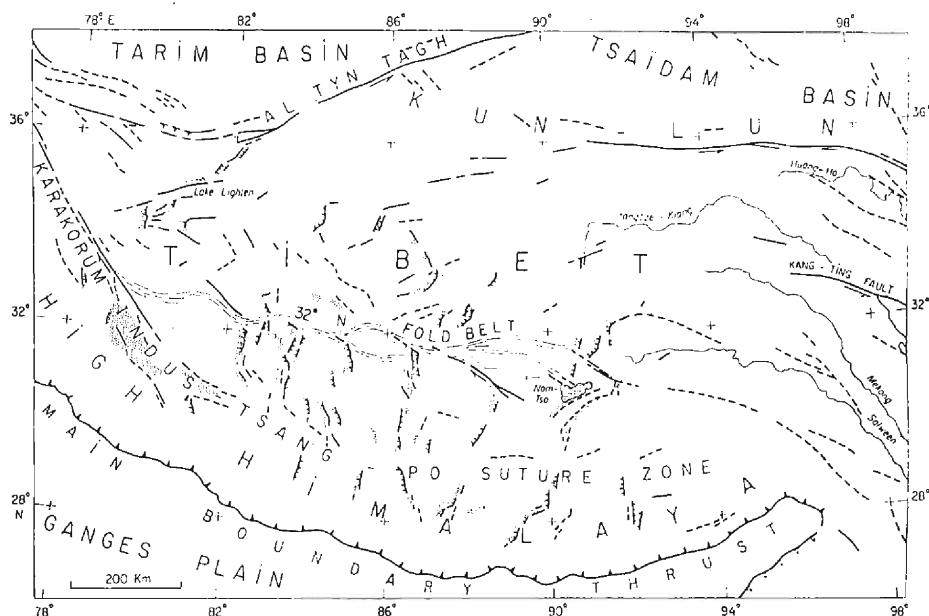


Fig. 13. Simplified map of active tectonics in the Tibet and its surrounding regions. Heavy lines are faults recognized LANDSAT imagery. Dotted areas are sediment-filled basins due to normal faulting. North-south normal faulting appears to be the dominant mode of present crustal deformation within the Tibet Plateau (after Molnar, 1978<sup>20</sup>).

crevices in the Tibet plateau. They and the extensional (N-S) graben known as "boudinage structure" in the Tibetan plateau reported by Froidevaux and Ricard (1987) are geological evidences of the existence of an extensional active tectonic system in the Tibet region.<sup>25)</sup>

**Fig. 14** and **Fig. 15** respectively show the distributions of crustal thickness and of Bouguer anomalies of gravity in China (Feng, 1985).<sup>26)</sup> From these figures, the crustal thickness of the Tibetan plateau is calculated to be from 50 km to 68 km and the negative Bouguer anomalies are large down to  $-500$  mgal throughout the whole region. Furthermore this region almost corresponds with the region where our results show that normal fault type events are predominant.

On the other hand, in the Tibetan plateau, there are anomalous geothermal regions in which more than 600 hot springs have been discovered, and the temperature of some of them is over the boiling point. In the northern margin of the Tibetan plateau, a volcanic eruption took place at the south Yutian county of Xinjiang province on October 27, 1951 (Tong et al., 1981). These volcanoes are located on the northern edge of the region where there are a lot of normal faults (**Fig. 16**).<sup>27,30)</sup> This is also a region where a distinct low- $Q$  value was found in the crust (Feng et al. 1980, Teng et al. 1980).<sup>28,29)</sup> From the study of satellite data and surface gravity data, Liu (1978) suggested that the tensile stresses caused by the upward mantle convection

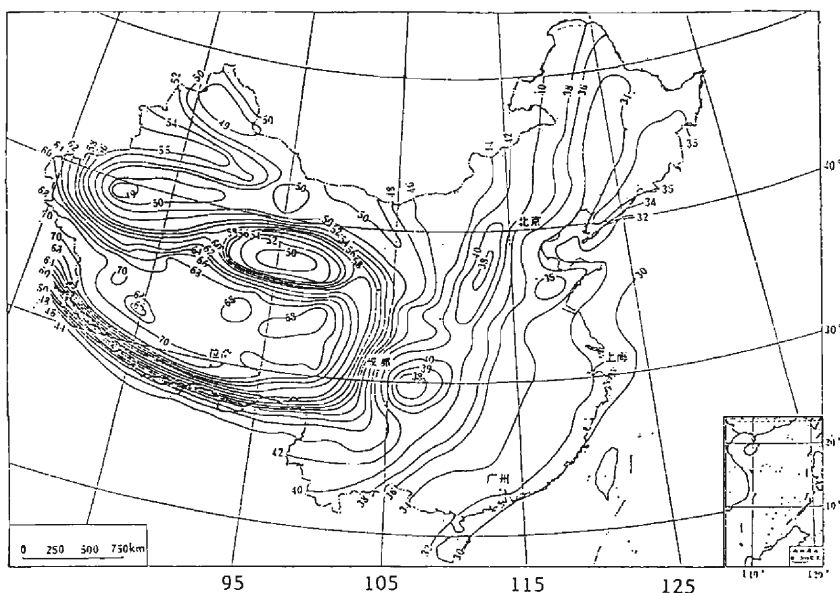


Fig. 14. Crustal thickness in China (unit: km) (after Feng, 1985<sup>26</sup>).

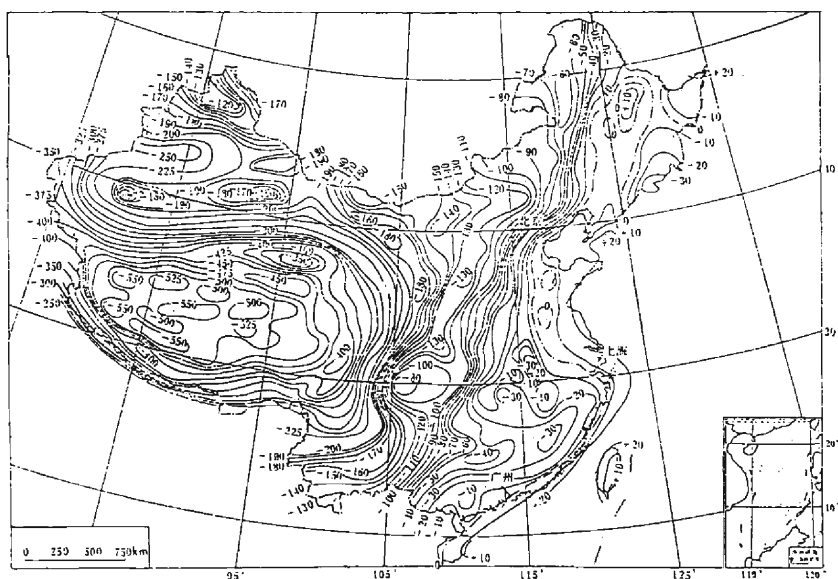


Fig. 15. Bouguer gravity anomalies in China (unit: mgal) (after Feng, 1985<sup>26</sup>).

flows under the crust is acting in the Tibetan region (**Fig. 16**).<sup>30</sup> These results are also consistent with our results which shows that normal faulting events occur in this region.

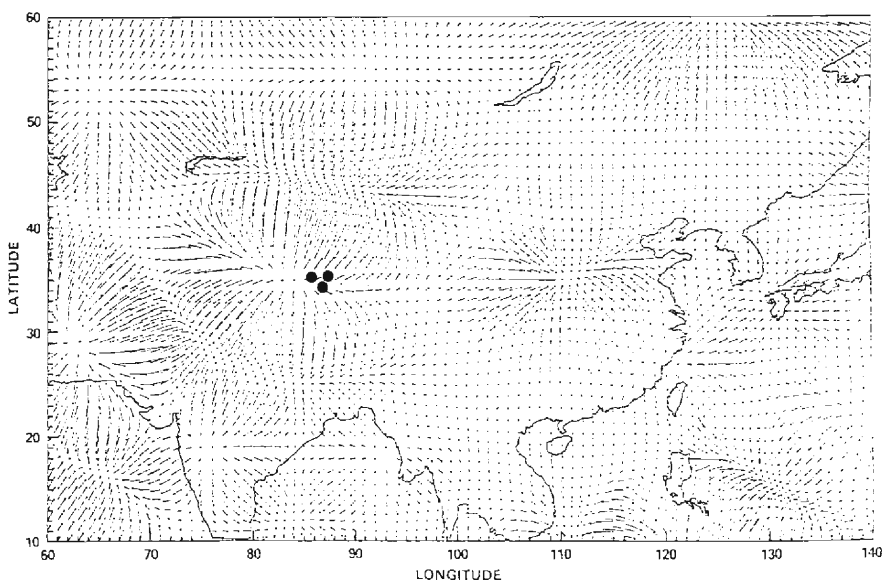


Fig. 16. Subcrustal stress exerted by mantle convection under Asia and volcanoes in West China (after Liu, 1978<sup>30)</sup>). Three closed circles shows active volcanoes.

The wide distribution of compressive stress fields in the West China region has been confirmed, and the existence of an extensional stress field in the western and central area of the Tibetan plateau has been clarified from new focal mechanism data obtained in this study. Various kinds of geological and geophysical data and some theoretical calculations by the preceding studies are consistent with the result from focal mechanism data. It is important to observe small earthquakes for further detailed studies of fine tectonic structure in this region.

### Acknowledgment

We wish to express our thanks to Dr. K. Matsumura for providing valuable data and his kind help. Data were processed on the FACOM-M340R of the Information Data Processing Center for Disaster Prevention Research, Disaster Prevention Research Institute, Kyoto University.

### References

- 1) Huan, W.L., Z.L. Shi, J.Q. Yan and S.Y. Wang: Characteristics of the Recent Tectonic Deformation of China and Its Vicinity, *Acta Seismologica Sinica*, Vol. 1, No. 2, 1979, pp. 109-120 (in Chinese).
- 2) Teng, J.W., S.Y. Wei, K.Z. Sun and G.S. Xue: The Characteristics of the Seismic Activity in the Qinghai-Xizang (Tibet) Plateau of China, *Tectonophysics*, 134 (1987), pp. 129-144.
- 3) Shi, Z.L., W.L. Huan, S.D. Lu and J.Q. Yan: On the Characteristics of Seismic Activity in Central and Eastern Asia Continent, *Scientia Sinica (series B)*, Vol. XXVI, No. 4, 1983, pp. 438-448.

- 4) Oike, K.: Seismic Activity in the Eastern Asia, Orogenic Belt in the Asia—from Himalaya to Japan Trench—, Editor by K. Huzita, Kaibendo, 1984, pp. 89–107 (in Japanese).
- 5) Tapponnier, P. and P. Molnar: Active Faulting and Tectonics in China, *J. Geophys. Res.*, 82 (20), 1977, pp. 2905–2930.
- 6) Valdiya, K.S.: Tectonics of the Central Sector of the Himalaya, in Zagros, Hindu kush, Himalaya-Geodynamic Evolution, *Geodyn. Ser. Vol. 3*, edited by H.K. Gupta and F.M. Delany, pp. 87–110, AGU, Washington, D.C., 1981.
- 7) Ni, J. and M. Barazangi: Seismotectonics of the Himalayan Collision Zone: Geometry of Underthrusting Indian Plate Beneath the Himalaya, *J. Geophys. Res.*, Vol. 89, No. B2, 1984, pp. 1147–1163.
- 8) Lyon-Caen, H. and P. Molnar: Constraints on the Structure of the Himalaya from an Analysis of Gravity Anomalies and A Flexural Model of the Lithosphere, *J. Geophys. Res.*, Vol. 88, No. B10, 1983, pp. 8171–8191.
- 9) Khattri, K.N.: Great Earthquakes, Seismicity Gaps and Potential for Earthquake Disaster along the Himalaya Plate Boundary, *Tectonophysics*, 138 (1987), pp. 79–92.
- 10) Zhao, Z.X., K. Matsumura, K. Oike and Y. Ishikawa: Regional Characteristics of Temporal Variation of Seismic Activity in East Asia and Their Mutual Relation (3) Regions in West China and Its Neighbor Regions, *Zisin* (in press) (in Japanese).
- 11) Zonenshain, L.P. and L.A. Savostin: Geodynamics of the Baikal Rift Zone and Plate Tectonics of Asia, *Tectonophysics*, 76 (1981), pp. 1–45.
- 12) Verma, R.K. and G.V.R. Krishna Kumar: Seismicity and the Nature of Plate Movement along the Himalayan Arc, Northeast India and Arakan-Yoma: A Review, *Tectonophysics*, 134 (1987), pp. 153–175.
- 13) Oike, K.: On the Nature of Seismic Activity in the Eastern Asia, A Collection of Papers of International Symposium on Continental Seismicity and Earthquake Prediction, Seismological Press, Beijing, China, 1984, pp. 78–87.
- 14) Ishikawa, Y.: The Tectonics in the Eastern Asia (2), Program and Abstracts, *Seism. Soc. Japan*, 1986, No. 2, pp. 35 (in Japanese).
- 15) Yan, J.Q., Z.L. Shi, S.Y. Wang and W.L. Huan: Some Features of the Recent Tectonic Stress Field of China and Environs, *Acta Seismologica Sinica*, Vol. 1, No. 1, 1979, pp. 9–24 (in Chinese).
- 16) Aki, K.: Earthquake Generating Stress in Japan for the Years 1961 to 1963 Obtained by Smoothing the First Motion Radiation Patterns, *Bulletin of the Earthquake Research Institute*, Vol. 44 (1966), pp. 447–471.
- 17) Oike, K.: On the Nature of the Occurrence of Intermediate and Deep Earthquakes. 1. The World Wide Distribution of the Earthquake Generating Stress, *Bulletin of the Disaster Prevention Research Institute, Kyoto University*, Vol. 20, 1971, pp. 145–182.
- 18) Ishikawa, Y.: Tectonics of East Asia Inferred from Seismicity and Focal Mechanism of Earthquakes, 1988, (in preparation).
- 19) Otsuki, K.: Plate Tectonics of Eastern Eurasia in the Light of Fault Systems, *Science Reports of the Tohoku University, Sendai, Second Series (Geology)*, Vol. 55, No. 2, 1985, pp. 141–251.
- 20) Molnar, P. and P. Tapponnier: Active Tectonics of Tibet, *J. Geophys. Res.*, Vol. 83, No. B11, 1978, pp. 5361–5375.
- 21) Ni, J. and J.E. York: Late Cenozoic Tectonics of the Tibetan Plateau, *J. Geophys. Res.*, Vol. 83, No. B11, 1978, pp. 5377–5384.
- 22) Molnar, P. and W.P. Chen: Focal Depth and Fault Plane Solutions of Earthquakes under the Tibetan Plateau, *J. Geophys. Res.*, Vol. 88, No. B2, 1983, pp. 1180–1196.
- 23) Deway, J.F and J.M. Bird: Mountain Belts and New Global Tectonics, *J. Geophys. Res.*, Vol. 75, 1970, pp. 2625–2647.
- 24) Minster, Y., T. Yordan, P. Molnar and E. Haines: Numerical Modeling of Instantaneous Plate Tectonics, *Geophys. J.R. Astron. Soc.*, 36, 1974, pp. 541–576.
- 25) Froidevaux, C. and Y. Ricard: Tectonic Evolution of High Plateaus, *Tectonophysics*, 134 (1987), pp. 227–238.
- 26) Feng, R.: Crustal Thickness and Densities in the Upper Mantle beneath China—the Results

- of Three Dimensional Gravity Inversion, *Acta Seismologica Sinica*, Vol. 7, No. 2, 1985, pp. 143–157 (in Chinese).
- 27) Tong, W., Z.F. Zhang, Z.J. Liao, M.X. Zhu and M.T. Zhang: Hydrothermal Activities Occurring in Xizang (Tibetan) Plateau and Preliminary Discussion About the Thermal Region within Its Upper Crust, *Acta Geophysica Sinica*, 1982, Vol. 25, No. 1, pp. 34–40 (in Chinese).
- 28) Feng, R., and Z.Q. He: Q-value for Surface Wave in the Eastern Region of Xizang Plateau, *Acta Geophysica Sinica*, 1980, Vol. 23, No. 3, pp. 291–297 (in Chinese).
- 29) Teng, J.W., S.Z. Wang, Z.X. Yao, Z.W. Xu, Z.W. Zhu, B.P. Yang and W.H. Zhou: Characteristics of the Geophysical Fields and Plate Tectonics of the Qinghai-Xizang Plateau and Its Neighboring Regions, *Acta Geophysica Sinica*, 1980, Vol. 23, No. 3, pp. 254–268 (in Chinese).
- 30) Liu, H.S.: Mantle Convection Pattern and Subcrustal Stress Field under Asia, *Phys. Earth Planet. Inter.*, 16, (1978), pp. 247–256.